



Cite this: *Sustainable Energy Fuels*,
2023, 7, 671

Supported rhenium catalysts for the hydrogenation of levulinic acid derivatives: limits and potential†

Riccardo Bacchicchi,^{ab} Jacopo De Maron,^{ab} Tommaso Tabanelli,^{id} *^{ab}
Daniele Bianchi^c and Fabrizio Cavani^{id} *^{ab}

Levulinic acid derivatives, such as alkyl levulinates, are suitable starting reactants for the production of fuel components, namely γ -valerolactone (GVL), alkyl valerates, pentanol, and pentylvalerate (PV). The reactions were performed in batch, without any additional solvents, by investigating the catalytic activity of several Re-based catalysts. In this way, we confirmed the crucial role of the support acidity in promoting the ring-opening of GVL and its consecutive reduction to valeric compounds. In the optimised conditions, bimetallic Re-Ru-O/HZSM-5 yielded methyl valerate (MV) and valeric acid (VA) with a productivity of 512 mmol g_{metal}⁻¹ h⁻¹, one of the highest reported in the literature to date. Rhenium can also foster the reduction of valeric acid/esters to PV through the formation of 1-pentanol and its efficient esterification/transesterification with the starting material. However, we also proved that Re-based catalysts undergo leaching of the active phase in the presence of carboxylic acids, especially by working in neat with VA, thus limiting the recyclability of the catalytic material. Furthermore, the over-reduction of rhenium affects catalytic performance, suggesting not only that a pre-reduction step is unnecessary, but also that it could be detrimental for the catalytic activity.

Received 15th November 2022
Accepted 10th January 2023

DOI: 10.1039/d2se01583h

rsc.li/sustainable-energy

1. Introduction

Starting from the industrial revolution, human activities have affected the carbon cycle not only by adding more carbon dioxide to the atmosphere, but also by affecting the ability of forests, soils, and oceans to capture and store CO₂ from the air.¹ Lignocellulosic biomass (LCB) is one of the most abundant renewable feedstocks and may replace fossil raw materials in chemical and fuel production.^{2,3} For instance, the pyrolysis of LCB can yield a bio oil containing carboxylic acids that can be upgraded to gasoline by means of a ketonization/hydrotreating process.⁴ Alternatively, LCB can be used to produce several significant building blocks such as syngas (by means of gasification), methanol (from syngas), ethanol (by glucose fermentation), and ethylene (by ethanol dehydration). These molecules can be further combined to produce valuable bio-based chemicals, such as methyl methacrylate.⁵ Among the bioderived platform molecules obtainable from LCB, levulinic acid (LA) was selected by the U. S. Department of Energy as one of the top twelve most valuable molecules and with the greatest potential, with a market value of approximately 4000 Tonnes per year in

2020.^{6,7} In particular, the most investigated strategy for the exploitation of LA is its hydrogenation towards fuel additives, solvents, and other added-value bio-based chemicals and, in this context, heterogeneous and homogeneous catalysts are widely used.⁸ In literature, most works deal with the conversion of LA and its ester towards γ -valerolactone (GVL) because LA is the most easily obtainable compound, either by hydrogenation with H₂ or by catalytic H-transfer hydrogenation with light, bio-based alcohols, in both liquid- and gas-phase continuous flow reactors.^{9–16}

The most recent advances in literature, however, have also led to different consecutive reduction products.¹⁷ For instance, 2-methyltetrahydrofuran (2-MTHF) was proposed as an efficient fuel additive for gasoline formulations and as an eco-friendly solvent alternative to THF.^{18–21} Another significant product is 1,4-pentadiol (1,4-PDO), thanks to its potential use as a renewable monomer for the production of polyesters.^{22,23} Lastly, the preparation of valeric acid and/or its esters (VA/VE) was reported over a variety of heterogeneous, bifunctional catalysts, in particular those combining a support displaying Brønsted acidity with an active (*i.e.* group VIII) hydrogenation metal.²⁴ The most promising results on this topic are reported in Table 1.^{25–31}

A high activity and selectivity towards VA/VE were reported for all catalysts, but in most cases both an additional organic solvent and a high molar excess of hydrogen were required, compared to LA. Furthermore, some authors reported leaching issues (*e.g.* dealumination or desulfurization of the support)

^aDipartimento di Chimica Industriale Toso Montanari, Università di Bologna, Viale Risorgimento 4, 40136 Bologna, Italy. E-mail: tommaso.tabanelli@unibo.it

^bCenter for Chemical Catalysis-C3, Alma Mater Studiorum Università di Bologna, Viale Risorgimento 4, 40136 Bologna, Italy

^cIstituto Eni Donegani, Via Fauser 4, 28100 Novara, Italy

† Electronic supplementary information (ESI) available. See DOI: <https://doi.org/10.1039/d2se01583h>



Table 1 Comparison between the most-performing catalysts in batch conditions for the hydrogenation of LA to VA/VE

Catalyst	Reaction condition				Conversion (%)	Yield (%)			Ref.
	Solvent	<i>T</i> (°C)	<i>P</i> _{H₂} (bar)	Time (h)		GVL	VA + VE	Other	
Ru/SBA-SO ₃ H	Ethanol	240	40	6	100	1	94	1	25
Ru/HZSM-5	1,4-Dioxane	200	40	10	100	8	91	—	26
Pd/HZSM-5	Ethanol	240	40	8	100	8	90	2	27
Co/HZSM-5	Ethanol	240	30	3	100	1	97	—	28
Ru/HZSM-5	1,4-Dioxane	220	30	10	100	1	86	—	29
Nb-Cu/ZPS	Water	150	30	4	100	—	99 ^a	—	30
Pt/HMFI	—	200	8	6	100	—	99 ^a	—	31

^a Only valeric acid.

which were often difficult to solve. As shown in Table 1, in the majority of works in literature dealing with LA hydrogenation, solvents were used (e.g. 1,4-dioxane, water, alcohols, long-chain hydrocarbons); some studies, however, showed promising results also with neat LA. For instance, Weckhuysen *et al.* obtained the complete conversion of LA yielding GVL by using Ru supported on TiO₂ and H-β as co-catalyst, while Shimizu *et al.* showed that Pt/HMFI is a suitable catalyst for the one-pot hydrogenation of LA to VA.^{31,32}

A much more challenging task is the selective reduction of the carboxylic group of LA and VA. In this context, bimetallic catalysts – in which one metal facilitates the heterolytic H₂ cleavage for hydrogenation/hydrogenolysis steps (e.g. Ru, Pt, Pd, Rh, Ir, Co, Ni, Cu), while the second metal (e.g. a promoter such as Sn, Mo, Cr, Re) fosters the activation/adsorption of the carbonyl group of the acid/ester molecule – are the most investigated, in many cases showing a substantial synergy.³³ Promoters are redox oxyphilic species which enhance the reducibility of carboxylic groups.³⁴ For instance, Toba *et al.* reported good results in the hydrogenation of mono- and dicarboxylic acids towards the corresponding alcohols and diols using a Ru-Sn-Al₂O₃ catalyst in a batch reactor (*i.e.* VA but not LA).³⁵ Li *et al.* hydrogenated acetic acid to ethanol at 100 °C over an Ir-MoO_x/SiO₂ catalyst on a tubular flow reactor.³⁶ A catalyst consisting of copper chromite mixed with an alkali or alkaline-earth metal component and an inorganic matrix component has been patented for the vapour-phase hydrogenation of methyl esters to fatty alcohols under fixed-bed conditions.³⁷ Davis *et al.* investigated the effect of ReO_x on the reduction of propionic acid over Pd-supported catalysts; likewise, Liang *et al.* studied the role of Re in Re-Ru/C bimetallic catalysts for the hydrogenation of succinic acid.^{38,39}

Several works suggest that the oxyphilic nature of rhenium is responsible for the interaction between active metal sites and carboxylic groups; however, Re may also activate H₂ by promoting dehydrogenation reactions;⁴⁰ hence, rhenium-based catalysts may selectively reduce carboxylic compounds. As an example, Toyao's group investigated the hydrogenation of aromatic carboxylic acids over a Re/TiO₂ catalyst, which selectively yielded the corresponding alcohols.⁴¹ Through density functional theory (DFT) calculations, they also demonstrated that Re and ReO_x showed a higher affinity towards carboxyl

groups as well as a lower affinity towards benzene moiety in comparison to other metal surfaces, thus proving that Re has an oxyphilic nature.^{42,43}

Compared to LA, levulinic esters (LE) can be obtained directly from cellulose by means of alcoholysis with good to excellent yields, without the need for a further esterification step, thus paving the way towards their direct exploitation as bio-based platform molecules.^{44–46} In particular, methyl, ethyl, and *n*-butyl levulinate are interesting thanks to their physico-chemical properties.⁴⁷ In fact, they might find applications not only as specialty chemicals, but also as additives in the fragrance and petrochemical industries.^{48–50} Moreover, LE are acid-free compounds and this makes them a promising alternative to levulinic acid as the starting material for the production of γ -valerolactone and its consecutive reduction products.^{51–54} In fact, the use of LA as reactant often causes the deactivation of the catalyst due to the leaching of the supported metal generated by acid media, and/or the fouling of the catalyst due to the oligomerization/polymerization of unsaturated intermediates.⁵⁵ Therefore, the catalytic conversion of LE might be more attractive for industrial applications.

To the best of our knowledge, there are no reports in literature on the direct hydrogenation of LA or LE to yield 1-pentanol (1-PAO). The properties of 1-PAO and its derivatives (*i.e.* dipentyl ether, pentyl valerate) make them suitable biofuels, thanks to their reduced particulate emissions and the consequent improvement in air quality.^{56–59} Pentyl valerate (PV) has appropriate polarities, better volatility, and higher ignition properties as a biofuel for gasoline and jet fuel applications.⁶⁰ In particular, the hydrogenation of GVL to PV in the liquid phase with pentanol as reactant/solvent has been investigated using noble metals supported on SiO₂-Al₂O₃- and Cu-based catalysts.^{61–65} The one-pot upgrading of GVL to PV was achieved with 60.6% of yield using a bifunctional 5% Pd/HY catalyst in a batch reactor system also without pentanol as reactant/solvent under relatively harsh conditions (260 °C, 80 bar of H₂, 30 h, solvent *n*-octane).⁶⁶

Herein, we report on the conversion of levulinic acid derivatives to 1-pentanol and/or pentyl valerate using a batch reactor in solvent-free conditions over Re-based catalysts. First, the hydrogenation of methyl levulinate (ML) was investigated in a one-pot approach aiming to directly obtain VA/VE, 1-PAO, and



PV. Then Re-based catalysts were examined also in the hydrogenation of valeric acid/ester (VA/VE) to evaluate the catalytic performance for the selective hydrogenation of carboxylic groups, with a special focus on both catalyst stability and the possible leaching of active species.

2. Experimental

All catalysts were prepared by incipient wetness impregnation (IWI) to obtain a 5 wt% rhenium on supports. For the IWI procedure, an aqueous solution containing a proper amount of NH_4ReO_4 was loaded on the support powder (usually 1.9 g); then it was oven-dried at 120 °C for 4 h and calcined at 500 °C for 3 h (ramp 5 °C min^{-1}) in static air to remove NH_4 ions and H_2O from the precursor and support. For the reduction step, the powder was exposed to an H_2/N_2 flow (100 ml min^{-1} , 10 vol% of H_2) at 350 °C for 1 h (ramp 10 °C min^{-1}). For the preparation of bimetallic catalysts, the NH_4ReO_4 solution was loaded first (in order to obtain a 5 wt% of Re on the support) and the sample was oven-dried at 120 °C before loading a solution of $\text{RuCl}_3 \cdot \text{H}_2\text{O}$ (to obtain 1 wt% of Ru on support). Silica and zeolite supports were delivered respectively by GRACE and Zeolyst (see ESI†).

Catalytic tests, the analysis system of post-reaction solutions, and the calculations for conversion, yields, and molar balance are described in detail in the “Experimental” section of the ESI.† The catalysts were characterized by means of N_2 -physisorption at 77 K with the BET method, MP-AES, XRD, TPR, and ATR-IR. Instrument specifications and analysis procedures are described in detail in the “Catalyst’s characterization” section of the ESI.†

In most research described in literature, the precursor used for the synthesis of Re-based catalysts is NH_4ReO_4 , for which XPS and XANES analyses confirm that the oxidation state of rhenium remains +7 after thermal treatment.^{43,67} Since all calcinations in this study were obtained in static air, it has been assumed that the Re oxidation state was not affected and that – as a consequence of the thermal treatment in the air – all NH_4ReO_4 was decomposed into Re_2O_7 . For the sake of simplicity, “ Re_2O_7 /support catalyst” has been shortened to “Re-O/support”.

3. Results and discussion

3.1 Supported Re–O catalysts

First, we investigated the effect of the support on the catalytic activity of Re-based materials for the hydrogenation of methyl levulinates (ML) to GVL and other consecutive reduction products. In particular, Table 2 shows the performances of Re–O/ SiO_2 and Re–O/HZSM-5 at 210 °C and 40 bar of hydrogen for 4 h. As mentioned in the Experimental section in the ESI,† by working with neat methyl levulinate the molar ratio H_2/ML in the reaction system was equal to only 1.4; therefore, the reaction system needed hydrogen refilling to keep the overall pressure constant during tests and to make the occurrence of the desired consecutive reduction reactions possible. Interestingly, both catalysts were active for the target reaction, with Re–O/HZSM-5

Table 2 Catalyst screening for ML hydrogenation. Reaction conditions: solvent free, $T = 210$ °C, $P_{\text{H}_2} = 40$ bar, $t = 4$ h, catalyst loading = 5 wt% [$m_{\text{cat}}/m_{\text{ML}}$]

Catalyst	Conv. ML (%)	Yield (%)			
		GVL	MV + VA	2-MTHF	Others
Re–O/ SiO_2	72	66	—	<1	2
Re–O/HZSM-5	88	67	4	<1	7
Re–R/HZSM-5 ^a	40	16	2	—	11

^a Pre-reduced at 350 °C for 1 h.

showing a higher ML conversion than Re–O/ SiO_2 (88% and 72% respectively), whereas the GVL yield was around 66% in both cases. Remarkably, Re promoted the hydrogenation of the carboxylic group of GVL leading to 2-MTHF (obtained with an underestimated yield of around 1% due to its higher volatility during the depressurization of the autoclave after the reaction). On the other hand, the higher acidity of Re–O/HZSM-5 in respect to Re–O/ SiO_2 led to the formation of valeric acid and methyl valerate. These compounds may be obtained *via* two main pathways: (i) the hydrogenation of ML carbonyl group to 4-hydroxypentanoic acid/ester (4-HPA/E) followed by its further dehydration and the saturation of the resulting double bond, or (ii) the consecutive ring-opening and hydrolysis of GVL to 4-HPA/E, which may then follow the previous reaction pathway.

Starting from these results, it was decided to investigate the influence of a pre-reduction treatment on the catalytic activity. In literature, a pre-reduction treatment of Re-based materials is usually carried out with H_2 diluted in an inert gas (5–30 vol%) at 500 °C before testing the materials. It has been reported that bulk Re_2O_7 , when heated in a hydrogen atmosphere, sublimates at 180 °C before its reduction.⁶⁸ Conversely, when Re_2O_7 is mixed with Pt or Pd, a complete reduction to metallic Re occurs below 200 °C without any loss. Firstly, the stability of the supported Re-species upon thermal treatment was verified by means MP-AES of the calcined materials and results are reported in Table 1S.† The amount of rhenium measured this way was in good agreement with the expected value of 5 wt%, suggesting that the metal-support interaction stabilizes rhenium species. Then, a pre-reduction treatment was carried out at 350 °C under a flow of 10 vol% H_2 in N_2 on Re–O/HZSM-5 before catalytic testing. The reduced catalyst was labelled Re–R/HZSM-5. Surprisingly, the pre-reduction treatment caused a significant drop in both the catalytic activity and the selectivity: not only did ML conversion decrease from 88% to 40%, but also GVL yield dropped from 44% to 16%, while Others’ yields increased from 7% to 11% compared to the non-reduced Re–O/HZSM-5 material (“Others” include 2-MTHF, 4-HPA/E, and unidentified products). The GC-FID analysis of the reaction mixture revealed the presence of heavier, high-retention-time compounds. Unfortunately, GC-MS analysis did not clarify their structure, but it is known that GVL can undergo decarboxylation to produce unsaturated compounds, such as butenes or pentenoic species, which may oligomerize to heavy products.^{55,69}



All in all, the drop in conversion of ML and the different product distribution indicate that a catalyst's over-reduction is detrimental for catalytic performance, as observed also in other cases, *i.e.* in the hydrogenolysis of glycols to alcohols or alkanes (*e.g.* from glycerol to propanols).^{70–72} Therefore, the nature of the support seems to play a side role in catalytic activity, while ML conversion and GVL yield seem to be mainly influenced by the oxidation state of rhenium.

For this reason, the reducibility of catalysts was investigated by means of H₂-TPR. Fig. S2† shows the H₂-TPR profiles of Re–O/SiO₂ and Re–O/HZSM-5, which are characterized by H₂ consumption centred at 415 °C and 385 °C, respectively. The lower reduction in temperature displayed by Re–O/HZSM-5 may suggest either a better dispersion of Re-species, which results in a high active surface or, from another point of view, a weaker interaction in respect to the one between rhenium and SiO₂, which decreases the temperature required for Re reduction. For both samples, the molar ratio between the hydrogen consumed and Re₂O₇ was around 5. Assuming an initial Re oxidation state of +7 (see Experimental), the observed H₂ consumption means that the average oxidation state of rhenium species will be +2 in the reduced material. It should be noted that Re²⁺ oxides (namely ReO phases) are not stable and were only detected in particular conditions on rhenium-metal surfaces.⁷³ Conversely, rhenium usually forms oxides with oxidation states equal to +4, +6, and especially +7. Therefore, it may be argued that after reduction Re is more likely to be present as a mixture of metallic Re(0) and Re(IV) (ReO₂ phases), even though the presence of even higher oxidation states cannot be completely ruled out. The TPR characterization also showed that the reduction occurred in a single event and not in multiple steps, suggesting that the formation of reduced species such as Re(0) may generate a further reduction of the surrounding oxide, possibly by H₂ spillover, so that the reduction of Re⁷⁺ all the way down to Re(0) occurred within a very narrow temperature range.

Re–O/HZSM-5 was then selected for an investigation of the effect of temperature on the hydrogenation of ML, because this catalyst showed the highest activity toward the consecutive reduction products of GVL. The results of these tests are

reported in Fig. 1. At 180 °C, ML conversion was below 40%, the main product was GVL, and no traces of valeric acid or its ester were detected. Increasing the temperature from 180 °C to 210 °C led to more than twice as much ML conversion and triple the GVL yield, while valerates (MV and VA) also started to form. Remarkably, a further increase in temperature up to 230 °C did not lead to substantial differences in product distribution. The molar balance was good in all the temperature ranges investigated (>86%), demonstrating that the formation of heavy compounds was limited even by working in neat conditions. A qualitative analysis of the gaseous phase in GC-MS (Fig. S3a†) revealed the presence of light products such as methane, CO₂, and especially dimethyl ether (DME). Significantly, methyl pentyl ether (MPE), also, was detected in the gas phase using Re–O/HZSM-5. This is indirect evidence that Re, if combined with a support showing Brønsted acid sites, may catalyse the reduction of ML to the corresponding alcohol. In fact, it is well known that strong Brønsted acidic sites such as those shown by the HZSM-5 support catalyse the dehydration/condensation of alcohols.⁷⁴ As previously mentioned, the initial molar ratio H₂/ML in the reaction system is equal to only 1.4; therefore, the reaction system needed hydrogen refilling to (i) keep the total pressure constant at 40 bar during the tests, and (ii) make the desired consecutive reduction reactions possible. Nevertheless, the production of light, volatile compounds – mainly DME (bp –24 °C at atmospheric pressure), but also MPE – led to a further increase of the internal pressure, thus limiting or even hindering the addition of more molecular hydrogen, which is crucial for promoting further reductions. This was confirmed by the calculations (detailed in ESI†) of both hydrogen conversion (H₂ conversion) and methanol balance (MeOH balance), whose trends as a function of the reaction temperature are reported in Fig. S4.† Interestingly, H₂ conversion increased threefold when the temperature was increased from 180 °C up to 210 °C. However, it remained almost stable with a further increase up to 230 °C. At the same time, MeOH molar balance trends (related to liquid-phase products) showed a dramatic temperature-related decrease from 85% at 180 °C to 30% at 230 °C. MeOH missing from the balance was supposed to form the DME found among gaseous products by GC-MS. These results suggest that a significant partial pressure of DME in the headspace of the autoclave affected the hydrogen refilling by limiting the amount of H₂ that could be added. This is likely to be the reason why the results obtained at 230 °C are comparable to what was observed at 210 °C.

3.2 Supported Ru-Re-O catalysts

In the attempt to further improve catalyst performance, it was decided to combine a hydrogenation metal (Ru) with our main active metal (Re), by preparing a bimetallic system (Re–Ru–O/HZSM-5, 5 wt% Re and 1 wt% Ru), which was investigated in different reaction conditions for the hydrogenation of ML.

The influence of H₂ pressure has been investigated by means of experiments in the 10-to-40 bar pressure range: the results can be found in the “Effect of hydrogen pressure on catalytic activity” section of the ESI (Fig. S5†). Briefly, it was found that

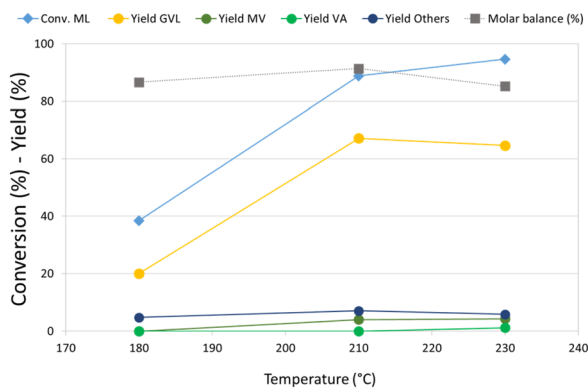


Fig. 1 Effect of temperature on ML hydrogenation over Re–O/HZSM-5. Reaction conditions: solvent free (ML neat), T = variable, P_{H_2} = 40 bar, t = 4 h, catalyst loading = 5 wt% [$m_{\text{cat}}/m_{\text{ML}}$]. Others = 2-MTHF, 4-HPA/E and unidentified products.



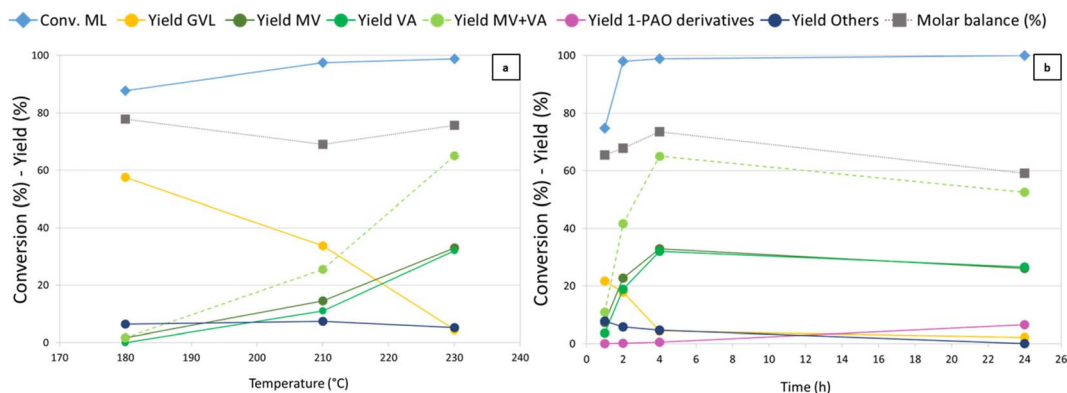


Fig. 2 ML hydrogenation over Re-Ru-O/HZSM-5. Reaction conditions: solvent free (ML neat), $P_{H_2} = 40$ bar, catalyst loading = 5 wt% [m_{cat}/m_{ML}]. (a) Effect of temperature for a 4 h reaction time and (b) effect of reaction time at 230 °C. Others = 2-MTHF, 4-HPA/E and unidentified products.

working at 40 bar was beneficial for the desired reaction and the all the following catalytic tests were carried out at this pressure.

Temperature (Fig. 2) was found to have a crucial influence on the reaction outcome, as shown in Fig. 2a. Thanks to its higher hydrogenating activity, at 180 °C Re-Ru-O/HZSM-5 showed results similar to those observed with Re-O/HZSM-5 at 230 °C. An increase in temperature up to 210 °C yielded up to 17% and 8% of MV and VA, while at the same time GVL yield decreased from 59% to 34%. A further increase in temperature boosted consecutive reductions and MV + VA were obtained with 65% yield, while GVL yield dropped to 5%. Notably, during tests over Re-Ru-O/HZSM-5 it was possible to refill hydrogen without interruption thanks to the enhanced hydrogenating activity of the catalyst, which competes kinetically with the acid-catalysed condensation of alcohols (particularly methanol) that was favoured at high temperature with Re-O/HZSM-5. The molar balance not exceeding 80% is probably due to the formation of over-reduction products such as light hydrocarbons. Indeed, a qualitative GC-MS analysis of the headspace detected light products such as methane, CO₂, DME, but also products of ML reduction such as MPE, MV, *n*-butane, and *n*-pentane (Fig. S3b†). Finally, Others' yield (including unidentified heavy products, 2-MTHF, methyl 4-hydroxypentanoate, and traces of methyl pentyl ether (MPE) and pentyl valerate (PV)) remained constant with temperature at around 7%. Time-resolved experiments were carried out at 230 °C under 40 bar of H₂ pressure (Fig. 2b) to assess the feasibility of promoting consecutive reduction reactions toward 1-pentanol and pentyl valerate. A ML conversion as high as 75% was achieved after only 1 h of reaction, and further increased (up to over 99%) after 2 hours already. Initially, GVL was the main product with a 22% yield after 1 hour, but it was replaced by valerates already after 2 hours (MV and VA). MV and VA were detected already after 1 h, and their yield increased over time, reaching a peak of 65% after 4 h, underlining the significant activity of the catalyst in the reduction of the so-formed hydroxy acid/ester to valerates. At the same time, it becomes evident that valerates may be further converted to consecutive products such as 1-pentanol, methyl pentyl ether, and pentyl valerate (grouped together under the term "1-pentanol derivatives = 1-PAO derivatives"), obtained

with a yield of 6% after 24 h. Products of valerates reduction were observed in gas-phase qualitative GC-MS analysis as well (Fig. S3c†). This finding, together with the worsening of the molar balance between 4 h and 24 h of reaction, suggests that the formation of gaseous products causes a decrease in the total yield of liquid phase products over time, leading to the observed decrease of the molar balance. The comparison of the catalytic activity of Re-O/HZSM-5, Ru-O/HZSM-5 and Re-Ru-O/HZSM-5 at optimised conditions (230 °C, 4 h, 40 bar of H₂) are shown in Fig. S9† again proving the beneficial effect of the co-presence of both Re and Ru in order to improve both MV + VA yields and molar balances.

3.3 Characterisation of Re-Ru-O/HZSM-5 catalyst

The reducibility of Re-Ru-O/HZSM-5 before and after reaction was characterized by means of TPR (Fig. S6†) and compared to the one of their monometallic analogues (Fig. S2†). The Re-O/HZSM-5 catalyst showed only one sharp peak at 380 °C, whereas the bimetallic Re-Ru-O/HZSM-5 showed one main reduction peak centred at 255 °C and a small one at 166 °C. These temperature correspond to the reduction of the Re and Ru oxide species respectively, as explained by Baranowska *et al.*⁷⁵ In their study, these authors investigated bimetallic Ru-Re/Al₂O₃ with different Ru/Re ratios (*i.e.*, 90/10, 75/25, 50/50) and found that Ru is reduced at lower temperature than Re; moreover, the presence of increasingly high amounts of Ru progressively reduces the temperature required by Re reduction. Hence, the sharp peak at 166 °C in the H₂-TPR profile for the fresh Re-Ru-O/HZSM-5 can be attributed to the reduction of the Ru species, which subsequently foster rhenium reduction at a lower temperature (255 °C) than the one required by Re-O/HZSM-5 (380 °C) by means of H₂ spillover. Similarly, the Re-Ru-O/HZSM-5 catalysts after ML hydrogenation under 40 bar of H₂ at 230 °C for 4 h, showed a broad reduction peak at 260 °C and a sharp peak at 115 °C (Fig. S6b†). Again, the hydrogen consumption during the analysis was measured, and for the freshly calcined Re-Ru-O/HZSM-5 it was assumed that all Ru was present as RuO₂ and that all Re was in *a + 7* initial oxidation state. Under these assumptions, after the complete reduction of



Ru(IV) to Ru(0), the molar ratio between the remaining consumed H₂ and the supported Re₂O₇ was around 5, suggesting that – as it was for Re–O/HZSM-5 – Re is present as a mixture of Re⁰ and ReO₂ after reduction. Conversely, during the reduction of the spent Re–Ru–O/HZSM-5, a much lower amount of hydrogen was consumed. In particular, the molar ratio H₂/(Re + Ru) was 5 times lower than for the fresh catalyst, thus suggesting that the supported Re₂O₇ and RuO₂ were partially reduced *in situ* to Ru(0) and Re(0) during the reaction with ML.

This high degree of reduction adversely affects catalyst performances as demonstrated by a catalytic test carried out over Re–Ru–R/HZSM-5 (the pre-reduction treatment was carried out at 350 °C under a flow of 10 vol% H₂ in N₂ on Re–Ru–O/HZSM-5 before the catalytic test, Fig. S7†). The relevant results showed the same trend as that observed for monometallic Re supported on HZSM-5. In fact, the performance of the pre-reduced bimetallic catalysts was worse than the one of the same freshly calcined material: ML conversion was 83%, GVL yield was 69%, and only 7% of MV + VA yield was obtained under the same reaction conditions.

In consideration of the information collected so far, we calculated the valeric acid/esters productivity of our catalyst in the best conditions and compared it with the values reported by other authors in literature (Table 3). Among the studies which employed a solvent and focused on the hydrogenation of LA (Table 3, entry 1–6), 2 wt% Pd/HZSM-5 showed high yield (90%) in VA + VE at 240 °C for 8 h in ethanol, but also high productivity, around 495 mmol_{VA+VE} g_{Pd}⁻¹ h⁻¹ (Table 3, entry 3).²⁷ Indeed, to the best of our knowledge, the direct HDO of neat ML to valeric acid/esters has been reported for the first time in the present work, with a VA + VE yield of 65% achieved with a bimetallic catalyst containing 5 wt% Re and 1 wt% Ru supported over HZSM-5, after a 4 h reaction at 230 °C, corresponding to a productivity of 512 mmol_{VA+VE} g_{Re+Ru}⁻¹ h⁻¹ (Table 3, entry 9). This productivity is comparable to that of catalysts which work with solvent, and it is at least threefold higher than the highest VA + VE productivity of 169 mmol_{VA} g_{Pd}⁻¹ h⁻¹ reported by Shimidzu *et al.* (Table 3, entry 7).³¹ Conversely, when

only Ru is considered as the active metal for hydrogenation, the corresponding productivity increased up to 3073 mmol_{VA+VE} g_{Ru}⁻¹ h⁻¹. As a matter of fact, only He *et al.* have recently reported a higher productivity, equal to 11 514 mmol_{VA+VE} g_{Ru}⁻¹ h⁻¹, by working at 220 °C with 40 bar of H₂ using 1 wt% Ru/HZSM-5 over neat ethyl levulinate (EL), this being the highest productivity reported to date.⁷⁶

3.4 VA and MV hydrogenation

Considering the ability of Re-supported materials to effectively catalyse the formation of valerates starting from ML, we decided to focus our efforts on the hydrogenation of valerates (VA and MV) with the aim of promoting the formation of 1-pentanol (1-PAO) and/or pentyl valerate (PV) following a “two-step” strategy (namely from ML to VA/MV and then from VA/MV to 1-PAO derivatives).

Table 4 reports the catalytic activity of bimetallic materials (*e.g.*, Re–Ru–O/HZSM-5 and Re–Ru–O/SiO₂), and monometallic materials (Re–O/SiO₂ and Re–O/HZSM-5) for VA hydrogenation at 210 °C, 40 bar of hydrogen, for 4 h. VA conversion was generally low, being the one obtained over Re–O/SiO₂ the highest (35%). Significantly, all materials displayed low selectivity to 1-PAO due to its consecutive fast esterification with excess VA that formed PV in its place (as also demonstrated later in this manuscript).

Notably, by carrying out the hydrogenation of neat VA, we were able to highlight a crucial issue which is often dramatically

Table 4 Catalyst screening for VA hydrogenation. Reaction conditions: solvent free (VA neat), *T* = 210 °C, *P*_{H₂} = 40 bar, catalyst loading = 5 wt% [*m*_{cat}/*m*_{VA}]

Catalyst	Conv. VA (%)	Yield (%)		Leaching Re (%)
		1-PAO	PV	
Re–O/SiO ₂	35	1	27	26.7
Re–Ru–O/SiO ₂	10	<1	7	30.5
Re–Ru–O/HZSM-5	17	0	7	42.9
Re–O/HZSM-5	15	<1	8	45.0

Table 3 Comparison of the productivity towards VA/VE in this work and reported in literature

Entry	Catalyst	Reaction conditions					Productivity (mmol _{VA+VE} g _{metal} ⁻¹ h ⁻¹)	Ref.
		Reactant	Solvent	<i>T</i> (°C)	<i>P</i> _{H₂} (bar)	Time (h)		
1	5 wt% Ru/SBA–SO ₃ H	LA	Ethanol	240	40	6	63	25
2	1 wt% Ru/HZSM-5	LA	1,4-Dioxane	200	40	10	391	26
3	2 wt% Pd/HZSM-5	LA	Ethanol	240	40	8	495	27
4	10 wt% Co/HZSM-5	LA	Ethanol	240	30	3	278	28
5	3 wt% Ru/HZSM-5	LA	1,4-Dioxane	220	30	10	115	29
6	4–40 wt% Nb–Cu/ZPS	LA	Water	150	30	4	39	30
7	5 wt% Pt/HMFI	LA	—	200	8	6	169	31
8	5–1 wt% Re–Ru–O/HZSM-5	ML	—	230	40	4	512	This work ^a
9	5–1 wt% Re–Ru–O/HZSM-5	ML	—	230	40	4	3073	This work ^b
10	1 wt% Ru/La–Y (or HY)	EL	—	220	40	0.5	11 514	76

^a Calculated considering all metal loading. ^b Calculated considering only Ru loading.



underrated in literature: rhenium leaching. Generally speaking, leaching of rhenium was higher for the HZSM-5-supported catalyst ($\approx 45\%$) than for the SiO_2 -supported catalyst (27–30%). Previously, it was suggested that the lower reduction temperature displayed by Re–O/HZSM-5 in respect to Re–O/ SiO_2 may indicate either a better dispersion of Re-species on the zeolite support, which results in a higher active surface, or else that the rhenium– SiO_2 interaction is stronger compared to Re–HZSM-5 (see Fig. S3, ESI†). In agreement with H_2 -TPR results, the lower leaching values for silica-supported catalysts may indicate that rhenium is more strongly bonded to SiO_2 than to HZSM-5.

Fig. 3 shows the catalytic results obtained in MV hydrogenation at 210 °C, 40 bar of hydrogen, for 4 h with Re–O/ SiO_2 and Re–O/HZSM-5. Over Re–O/ SiO_2 the conversion of MV and product yields were low ($X_{\text{MV}} \approx 15\%$, $\text{PV} = 7\%$ and $1\text{-PAO} = 1\%$), but the amount of Re lost due to leaching was very low as well (1.1%).

On the other hand, the performance of Re–O/HZSM-5 in the same conditions was quite different: in fact, MV conversion was as high as 50% and the main product was VA with a yield of 17%, while PV, 1-PAO, and methyl pentyl ether (MPE) were obtained in small amounts. As a consequence, the molar balance obtained was much lower than the one obtained with Re–O/ SiO_2 . This evidence suggests that during the hydrogenation of MV different supports foster different reaction pathways: for instance, the strongly acidic HZSM-5 trigger mainly the hydrolysis of MV to VA and other side reactions that worsen the molar balance by forming light incondensable compounds and/or heavy carbonaceous residues. At the same time, Re loss due to leaching with Re–O/HZSM-5 (5.6%) was higher than with Re–O/ SiO_2 .

Generally speaking, the use of MV as the reactant significantly reduces the leaching of Re for both Re–O/ SiO_2 and Re–O/HZSM-5 (see Table 4), strongly suggesting that VA is the main actor in the active-phase dissolution because of its acidic characteristics. In this context, the higher metal leaching suffered by the zeolite-supported catalyst can be explained by its high activity towards MV hydrolysis to VA.

MV hydrogenation was further investigated as a function of the reaction time over Re–O/ SiO_2 (Fig. 4).

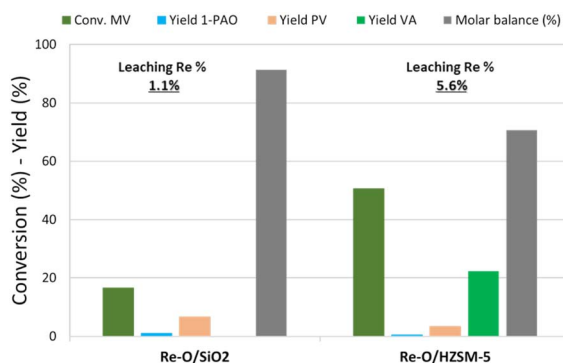


Fig. 3 MV hydrogenation over monometallic catalysts. Reaction conditions: solvent free (neat MV), $T = 210$ °C, $P_{\text{H}_2} = 40$ bar, $t = 4$ h, catalyst loading = 5 wt% [$m_{\text{cat}}/m_{\text{MV}}$]

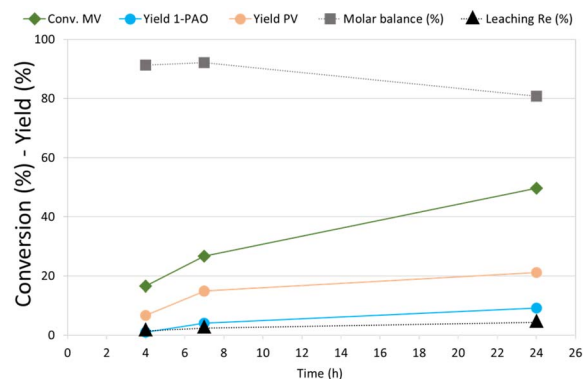


Fig. 4 Effect of reaction time in MV hydrogenation over Re–O/ SiO_2 . Reaction conditions: solvent free (neat MV), $T = 210$ °C, $P_{\text{H}_2} = 40$ bar, $t = 4$ h, catalyst loading = 5 wt% [$m_{\text{cat}}/m_{\text{MV}}$]

By increasing the reaction time from 4 to 7 h the conversion of MV increased from around 15% to 27%, while PV and 1-PAO yields, reached 15% and 4% respectively. Unfortunately, increasing further the reaction time to 24 h did not produce a proportional increase in the target products yield, ($\text{PV} = 21\%$ and $1\text{-PAO} = 10\%$) due to consecutive reactions that worsened the molar balance (81%). However, the leaching of rhenium (4.3%) was limited even after 24 h of reaction. As a matter of fact, VA was not detected among reaction products because the activity of Re–O/ SiO_2 for MV hydrolysis to VA is low: as a consequence, the loss of active phase was much lower than the one obtained during the hydrogenation of VA.

Since the progressive rhenium leaching may negatively impact the recyclability of the catalysts, Re–O/ SiO_2 was recovered by filtration, washed with acetone, dried and recycled for another run. Results obtained by working with both VA and MV after 4 h, at 210 °C and 40 bar of hydrogen are shown in Fig. S8.† Interestingly, when VA is used as reactant, the extensive leaching of Re (26.7%) results in a dramatic loss of activity of the recycled catalyst. On the other hand, when the hydrogenation is carried out on MV the leaching is strongly limited (1.1%) and the catalytic performance of the recycled is comparable to the one of the fresh catalyst. Moreover, in order to exclude the contribution of any homogenous rhenium species a dedicated Sheldon test was carried out during the hydrogenation of VA with Re–O/ SiO_2 and the outcome is reported in Fig. S9.† After 2 h of reaction the catalyst was removed by filtration from the reaction mixture and thereafter VA conversion remained constant during the following 2 h, suggesting that despite VA fosters extensive leaching of Re, the resulting soluble Re-species do not contribute to the overall catalytic activity.

3.5 The reaction network: reactivity of intermediates

The reaction mechanism of VA/VE over Re–O/ SiO_2 was investigated by loading intermediates and products under the previously investigated reaction conditions (210 °C, 4 h, 40 bar). Fig. 5 shows the results obtained by loading the autoclave with neat valeric acid, valeraldehyde, 1-pentanol and pentyl valerate, respectively. As previously seen, VA conversion yielded mainly PV with very low amounts of 1-PAO.



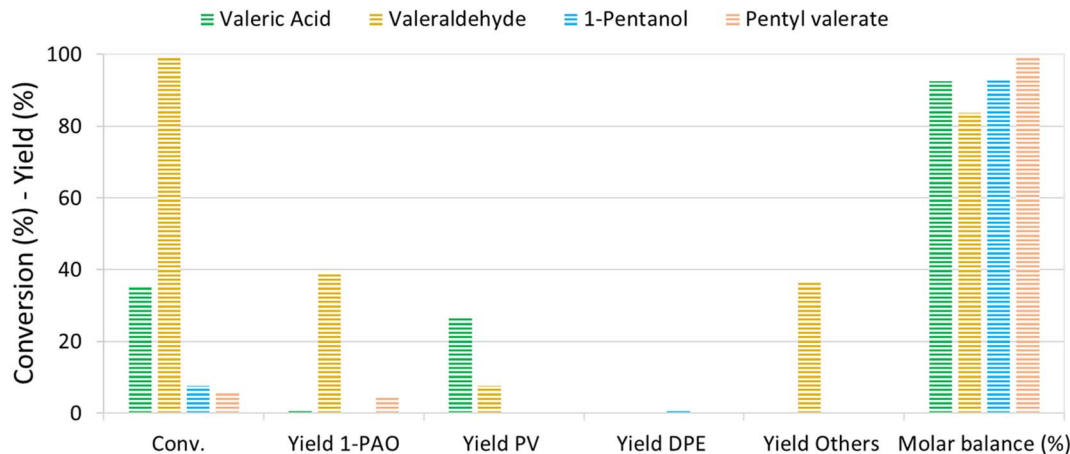


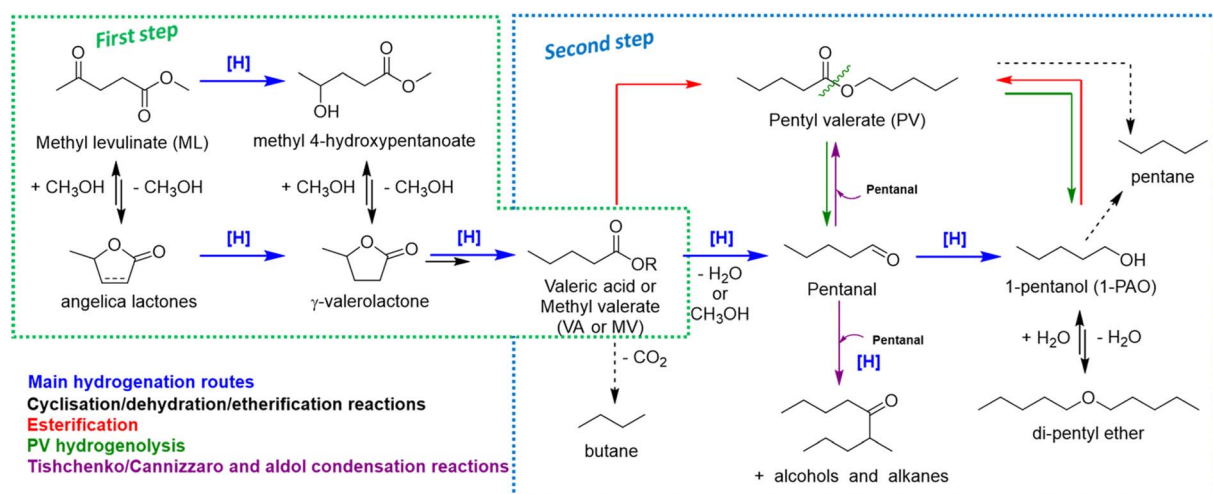
Fig. 5 Investigation of the reaction pathway loading intermediates and products in the presence of Re–O/SiO₂. Reaction conditions: solvent free, $T = 210\text{ }^{\circ}\text{C}$, $P_{\text{H}_2} = 40\text{ bar}$, $t = 4\text{ h}$, catalyst loading = 5 wt% [$m_{\text{cat}}/m_{\text{reactant}}$]

Interestingly, valeraldehyde showed a conversion >99%; 1-PAO yield was around 40%, whereas Others' yield reached 37%. Among Others, the compounds with longer carbon chains have been identified as C₁₀ aldehydes and alcohols formed *via* the aldolic condensations and hydrogenation of the obtained aldehydes; C₁₀ alkenes and alkanes were found too. PV was detected with a yield of 8% and was probably formed *via* a Cannizzaro-like disproportionation and consecutive esterification or directly *via* a Tishchenko reaction.

Interestingly, when 1-PAO was charged as reactant, proved to be a quite stable compound in the absence of strong Brønsted acidic sites over the catalyst, showing a conversion of only 7%. Likewise, PV showed a low conversion of about 6% and only 1-PAO was detected as the product. For each test, the headspace of the autoclave after reaction was analysed qualitatively by means of GC-MS: *n*-butane and *n*-pentane were detected in every test.

Summarizing all the information collected so far, the overall reaction scheme reported in Scheme 1 may be proposed.

During VA hydrogenation, valeric acid is partially reduced to highly reactive valeraldehyde (pentanal), even if it has not been detected, or partially decomposed through decarboxylation reaction yielding *n*-butane (Scheme 1, second step). Under standard reaction conditions, valeraldehyde is an unstable intermediate which might react in several ways. Hydrogenation to 1-PAO is the main reaction obtained by working with a hydrogen excess and/or limited concentration of the aldehyde; however, by working in neat conditions, aldol condensation to C₁₀ aldehydes and alcohols and Tishchenko or Cannizzaro disproportion to PV were effectively induced. Indeed, when the aldehyde was formed as an intermediate (*i.e.*, starting from VA), no traces of C₁₀ were found in the liquid phase. PV may be formed through the esterification of VA with 1-PAO, but also *via* a Tishchenko or Cannizzaro reaction of valeraldehyde. With regard to 1-PAO, its stability lead consecutive hydrogenolysis reaction unfavourable, leading to only traces of *n*-pentane and di-pentyl ether (DPE). As a matter of fact, 1-PAO effectively reacted in the presence of VA to yield PV under these reaction



Scheme 1 Proposed reaction scheme from ML to 1-PAO derivatives through the formation of VA/MV.



conditions. Lastly, PV showed limited reactivity; the only detected product was 1-PAO. The absence of VA suggests that an important contribution of ester hydrolysis reaction back to VA and 1-PAO can be ruled out. Even in the case of MV, valeric acid was not detected in the reaction mixture, indicating that VA is not a crucial intermediate in alkyl valerate hydrogenation. These data suggest that alkyl valerate hydrogenolysis may occur by splitting into aldehyde and alcohol (green arrows). However, it cannot be ruled out that the splitting occurs between oxygen and the alkyl chain, yielding pentane and valeric acid; the latter can be converted as detailed above. Previous results of MV hydrogenation suggest that Re–O/SiO₂ mainly privileges the first pathway, whereas Re–O/HZSM-5 privileges the second one.^{77–79}

4. Conclusions

In summary, this work reports on the catalytic hydrogenation of levulinic acid derivatives, mainly methyl levulinate (ML), under H₂ atmosphere over supported Re-based catalysts without the need for any additional solvents. The nature of the support may lead to different reaction pathways. It has been suggested that rhenium over-reduction is detrimental to catalytic performance, but the influence and role of its oxidation state has not yet been fully elucidated.

With regard to the one-pot hydrogenation of ML to 1-PAO, bimetallic Re/Ru deposited on zeolite showed an interesting performance, leading to MV + VA yields of up to 65%; also, only traces of 1-PAO derivatives were found after 4 h at 230 °C. The calculated productivity of MV + VA in these conditions, at the best of our knowledge, was the second-highest ever reported in literature.

Considering that the increase of the reaction times only slightly increases the 1-PAO derivatives yield, a two-step approach for a more efficient production of these compounds has been proposed. Indeed, while in the first step MV/VA can be produced with an acceptable yield from ML, a second step for the further conversion of valeric compounds to 1-PAO, PV, or DPE has been investigated. We thus found that, starting from VA, a 27% PV yield could be achieved after 4 h at 210 °C. Nevertheless, an extensive rhenium leaching (of around 30–40%) has been observed with the use of neat VA. Interestingly, by working with MV, this issue can effectively be limited to below 4%, obtaining a PV yield of around 20% in the optimized condition over Re–O/SiO₂.

In the near future, further study will be crucial for highlighting the reaction mechanism over the surface and identifying an effective strategy for stabilizing Re species, thus increasing catalyst stability and recyclability.

Author contributions

Riccardo Bacchiocchi: conceptualization, methodology, investigation, validation, visualization, and writing – original draft. Jacopo De Maron: conceptualization, methodology, investigation, discussion and suggestions. Tommaso Tabanelli: conceptualization, investigation, validation, visualization, and

writing – review and editing. Daniele Bianchi: resources, discussion, funding acquisition, review and editing, and supervision. Fabrizio Cavani: conceptualization, resources, discussion, funding acquisition, review and editing, and supervision.

Conflicts of interest

There are no conflicts to declare.

Acknowledgements

Eni SpA is acknowledged for the PhD grant assigned to RB.

Notes and references

- 1 IPCC, *Climate Change 2014 Synthesis Report*, 2014.
- 2 F. H. Isikgor and C. R. Becer, *Polym. Chem.*, 2015, **6**, 4497–4559.
- 3 C. H. Zhou, X. Xia, C. X. Lin, D. S. Tong and J. Beltramini, *Chem. Soc. Rev.*, 2011, **40**, 5588–5617.
- 4 J. De Maron, L. Bellotti, A. Baldelli, A. Fasolini, N. Schiaroli, C. Lucarelli, F. Cavani and T. Tabanelli, *Sustainable Chem.*, 2022, **3**, 58–75.
- 5 J. De Maron, M. Eberle, F. Cavani, F. Basile, N. Dimitratos, P. J. Maireles-Torres, E. Rodriguez-Castellón and T. Tabanelli, *ACS Sustain. Chem. Eng.*, 2021, **9**, 1790–1803.
- 6 T. Werpy and G. Petersen, *Top Value Added Chemicals from Biomass*, 2004, **1**, 76.
- 7 V. Rajendaren, S. M. Saufi and M. A. K. M. Zahari, *Biomass Convers. Biorefin.*, 2022, DOI: [10.1007/s13399-022-03444-7](https://doi.org/10.1007/s13399-022-03444-7).
- 8 K. Yan, C. Jarvis, J. Gu and Y. Yan, *Renew. Sustain. Energy Rev.*, 2015, **51**, 986–997.
- 9 W. R. H. Wright and R. Palkovits, *ChemSusChem*, 2012, **5**, 1657–1667.
- 10 A. Hommes, A. J. ter Horst, M. Koeslag, H. J. Heeres and J. Yue, *Chem. Eng. J.*, 2020, **399**, 125750.
- 11 B. Malleshham, P. Sudarsanam, B. Venkata Shiva Reddy, B. Govinda Rao and B. M. Reddy, *ACS Omega*, 2018, **3**, 16839–16849.
- 12 A. M. R. Galletti, C. Antonetti, V. De Luise and M. Martinelli, *Green Chem.*, 2012, **14**, 688–694.
- 13 G. Grillo, M. Manzoli, F. Buccioli, S. Tabasso, T. Tabanelli, F. Cavani and G. Cravotto, *Ind. Eng. Chem. Res.*, 2021, **60**, 16756–16768.
- 14 P. Blair Vásquez, T. Tabanelli, E. Monti, S. Albonetti, D. Bonincontro, N. Dimitratos and F. Cavani, *ACS Sustain. Chem. Eng.*, 2019, **7**, 8317–8330.
- 15 T. Tabanelli, *Curr. Opin. Green Sustainable Chem.*, 2021, **29**, 100449.
- 16 T. Tabanelli, E. Paone, P. Blair Vásquez, R. Pietropaolo, F. Cavani and F. Mauriello, *ACS Sustain. Chem. Eng.*, 2019, **7**, 9937–9947.
- 17 S. Dutta and N. S. Bhat, *ChemCatChem*, 2021, **13**, 3202–3222.
- 18 V. Pace, P. Hoyos, L. Castoldi, P. Domínguez De María and A. R. Alcántara, *ChemSusChem*, 2012, **5**, 1369–1379.



- 19 I. Obregón, I. Gandarias, N. Miletic, A. Ocio and P. L. Arias, *ChemSusChem*, 2015, **8**, 3483–3488.
- 20 I. Obregón, I. Gandarias, M. G. Al-Shaal, C. Mevissen, P. L. Arias and R. Palkovits, *ChemSusChem*, 2016, **9**, 2488–2495.
- 21 Y. B. Huang, A. F. Liu, Q. Zhang, K. M. Li, W. B. Porterfield, L. C. Li and F. Wang, *ACS Sustain. Chem. Eng.*, 2020, **8**, 11477–11490.
- 22 T. Mizugaki, Y. Nagatsu, K. Togo, Z. Maeno, T. Mitsudome, K. Jitsukawa and K. Kaneda, *Green Chem.*, 2015, **17**, 5136–5139.
- 23 M. Li, G. Li, N. Li, A. Wang, W. Dong, X. Wang and Y. Cong, *Chem. Commun.*, 2014, **50**, 1414–1416.
- 24 Z. Yu, X. Lu, J. Xiong and N. Ji, *ChemSusChem*, 2019, **12**, 3915–3930.
- 25 T. Pan, J. Deng, Q. Xu, Y. Xu, Q. X. Guo and Y. Fu, *Green Chem.*, 2013, **15**, 2967–2974.
- 26 W. Luo, P. C. A. Bruijninx and B. M. Weckhuysen, *J. Catal.*, 2014, **320**, 33–41.
- 27 M. Muñoz-Olasagasti, A. Sañudo-Mena, J. A. Cecilia, M. L. Granados, P. Maireles-Torres and R. Mariscal, *Top. Catal.*, 2019, **62**, 579–588.
- 28 P. Sun, G. Gao, Z. Zhao, C. Xia and F. Li, *ACS Catal.*, 2014, **4**, 4136–4142.
- 29 Z. Yi, D. Hu, H. Xu, Z. Wu, M. Zhang and K. Yan, *Fuel*, 2020, **259**, 3–6.
- 30 N. Karanwal, D. Verma, P. Butolia, S. M. Kim and J. Kim, *Green Chem.*, 2020, **22**, 766–787.
- 31 K. Kon, W. Onodera and K. I. Shimizu, *Catal. Sci. Technol.*, 2014, **4**, 3227–3234.
- 32 W. Luo, U. Deka, A. M. Beale, E. R. H. Van Eck, P. C. A. Bruijninx and B. M. Weckhuysen, *J. Catal.*, 2013, **301**, 175–186.
- 33 M. Tamura, Y. Nakagawa and K. Tomishige, *Asian J. Org. Chem.*, 2020, **9**, 126–143.
- 34 J. Pritchard, G. A. Filonenko, R. Van Putten, E. J. M. Hensen and E. A. Pidko, *Chem. Soc. Rev.*, 2015, **44**, 3808–3833.
- 35 M. Toba, S. I. Tanaka, S. I. Niwa, F. Mizukami, Z. Koppány, L. Gucci, K. Y. Cheah and T. S. Tang, *Appl. Catal. Gen.*, 1999, **189**, 243–250.
- 36 Z. Wang, G. Li, X. Liu, Y. Huang, A. Wang, W. Chu, X. Wang and N. Li, *Catal. Commun.*, 2014, **43**, 38–41.
- 37 D. Tharuk and W. Carrick, Copper chromite hydrogenation catalysts for production of fatty alcohols, WO 2012/074841, 2012.
- 38 X. Di, C. Li, B. Zhang, J. Qi, W. Li, D. Su and C. Liang, *Ind. Eng. Chem. Res.*, 2017, **56**, 4672–4683.
- 39 J. D. Kammert, A. Chemburkar, N. Miyake, M. Neurock and R. J. Davis, *ACS Catal.*, 2021, **11**, 1435–1455.
- 40 M. L. Gothe, K. L. C. Silva, A. L. Figueredo, J. L. Fiorio, J. Rozendo, B. Manduca, V. Simizu, R. S. Freire, M. A. S. Garcia and P. Vidinha, *Eur. J. Inorg. Chem.*, 2021, **2021**, 4043–4065.
- 41 T. Toyao, S. M. A. H. Siddiki, A. S. Touchy, W. Onodera, K. Kon, Y. Morita, T. Kamachi, K. Yoshizawa and K. I. Shimizu, *Chem.–Eur. J.*, 2017, **23**, 1001–1006.
- 42 T. Toyao, S. M. A. H. Siddiki, Y. Morita, T. Kamachi, A. S. Touchy, W. Onodera, K. Kon, S. Furukawa, H. Ariga, K. Asakura, K. Yoshizawa and K. I. Shimizu, *Chem.–Eur. J.*, 2017, **23**, 14848–14859.
- 43 T. Toyao, K. W. Ting, S. M. A. H. Siddiki, A. S. Touchy, W. Onodera, Z. Maeno, H. Ariga-Miwa, Y. Kanda, K. Asakura and K. Ichi Shimizu, *Catal. Sci. Technol.*, 2019, **9**, 5413–5424.
- 44 Y. B. Huang, T. Yang, Y. T. Lin, Y. Z. Zhu, L. C. Li and H. Pan, *Green Chem.*, 2018, **20**, 1323–1334.
- 45 J. Zhang, S. Bin Wu, B. Li and H. D. Zhang, *ChemCatChem*, 2012, **4**, 1230–1237.
- 46 A. M. Raspolli Galletti, C. Antonetti, S. Fulignati and D. Licursi, *Catalysts*, 2020, **10**, 1–2.
- 47 H. Ariba, Y. Wang, C. Devouge-Boyer, R. P. Stateva and S. Leveneur, *J. Chem. Eng. Data*, 2020, **65**, 3008–3020.
- 48 A. Démolis, N. Essayem and F. Rataboul, *ACS Sustain. Chem. Eng.*, 2014, **2**, 1338–1352.
- 49 H. Joshi, B. R. Moser, J. Toler, W. F. Smith and T. Walker, *Biomass Bioenergy*, 2011, **35**, 3262–3266.
- 50 L. Negahdar, M. G. Al-Shaal, F. J. Holzhäuser and R. Palkovits, *Chem. Eng. Sci.*, 2017, **158**, 545–551.
- 51 H. Chen, Q. Xu, D. Zhang, W. Liu, X. Liu and D. Yin, *Renewable Energy*, 2021, **163**, 1023–1032.
- 52 Z. Yang, Y. B. Huang, Q. X. Guo and Y. Fu, *Chem. Commun.*, 2013, **49**, 5328–5330.
- 53 Y. Kuwahara, Y. Magatani and H. Yamashita, *Catal. Today*, 2015, **258**, 262–269.
- 54 D. Ren, X. Wan, F. Jin, Z. Song, Y. Liu and Z. Huo, *Green Chem.*, 2016, **18**, 5999–6003.
- 55 P. M. Ayoub and J.-P. Lange, Process for converting levulinic acid into pentanoic acid, WO 2008/142127, 2008.
- 56 L. Wei, C. S. Cheung and Z. Huang, *Energy*, 2014, **70**, 172–180.
- 57 N. Yilmaz and A. Atmanli, *Fuel*, 2017, **191**, 190–197.
- 58 J. Campos-Fernandez, J. M. Arnal, J. Gomez, N. Lacalle and M. P. Dorado, *Fuel*, 2013, **107**, 866–872.
- 59 M. Marchionna, R. Patrini, F. Giavazzi, M. Sposini and P. Garibaldi, *World Pet. Congr. Proc.*, 2000, **3**, 38–45.
- 60 J. P. Lange, R. Price, P. M. Ayoub, J. Louis, L. Petrus, L. Clarke and H. Gosselink, *Angew. Chem., Int. Ed.*, 2010, **49**, 4479–4483.
- 61 K. G. Martínez Figueredo, E. M. Virgilio, D. J. Segobia and N. M. Bertero, *Chempluschem*, 2021, **86**, 1342–1346.
- 62 K. G. Martínez Figueredo, D. J. Segobia and N. M. Bertero, *Energy Convers. Manag.*, 2022, **13**, 0–11.
- 63 K. G. Martínez Figueredo, E. M. Virgilio, D. J. Segobia and N. M. Bertero, *React. Chem. Eng.*, 2022, **7**, 1997–2008.
- 64 W. Li, Y. Li, G. Fan, L. Yang and F. Li, *ACS Sustain. Chem. Eng.*, 2017, **5**, 2282–2291.
- 65 C. E. Chan-Thaw, M. Marelli, R. Psaro, N. Ravasio and F. Zaccheria, *RSC Adv.*, 2013, **3**, 1302–1306.
- 66 K. Yan, T. Lafleur, X. Wu, J. Chai, G. Wu and X. Xie, *Chem. Commun.*, 2015, **51**, 6984–6987.
- 67 B. Rozmysłowicz, A. Kirilin, A. Aho, H. Manyar, C. Hardacre, J. Wärmå, T. Salmi and D. Y. Murzin, *J. Catal.*, 2015, **328**, 197–207.



- 68 C. Bolivar, H. Charcosset, R. Frety, M. Primet, L. Tournayan, C. Betizeau, G. Leclercq and R. Maurel, *J. Catal.*, 1975, **39**, 249–259.
- 69 J. Q. Bond, D. Martin Alonso, R. M. West and J. A. Dumesic, *Langmuir*, 2010, **26**, 16291–16298.
- 70 Y. Amada, Y. Shinmi, S. Koso, T. Kubota, Y. Nakagawa and K. Tomishige, *Appl. Catal. B Environ.*, 2011, **105**, 117–127.
- 71 M. Tamura, Y. Amada, S. Liu, Z. Yuan, Y. Nakagawa and K. Tomishige, *J. Mol. Catal. Chem.*, 2014, **388–389**, 177–187.
- 72 N. Ota, M. Tamura, Y. Nakagawa, K. Okumura and K. Tomishige, *ACS Catal.*, 2016, **6**, 3213–3226.
- 73 M. T. Greiner, T. C. R. Rocha, B. Johnson, A. Klyushin, A. Knop-Gericke and R. Schlögl, *Z. Phys. Chem.*, 2014, **228**, 521–541.
- 74 C. Bandinelli, B. Lambiase, T. Tabanelli, J. De Maron, N. Dimitratos, F. Basile, P. Concepcion, J. M. L. Nieto and F. Cavani, *Appl. Catal. Gen.*, 2019, **582**, 117102.
- 75 K. Baranowska, J. Okal and N. Miniajluk, *Catal. Lett.*, 2014, **144**, 447–459.
- 76 J. He, Z. Wu, Q. Gu, Y. Liu, S. Chu, S. Chen, Y. Zhang, B. Yang, T. Chen, A. Wang, B. M. Weckhuysen and T. Zhang, *Angew. Chem., Int. Ed.*, 2021, **60**(44), 23713–23721.
- 77 L. Chen, J. Fu, L. Yang, Z. Chen, Z. Yuan and P. Lv, *ChemCatChem*, 2014, **6**, 3482–3492.
- 78 M. W. Schreiber, D. Rodriguez-Niño, O. Y. Gutiérrez and J. A. Lercher, *Catal. Sci. Technol.*, 2016, **6**, 7976–7984.
- 79 J. Chen and Q. Xu, *Catal. Sci. Technol.*, 2016, **6**, 7239–7251.

